2014-01-1991
Published 04/01/2014

doi:10.4271/2014-01-1991
saetransaf.saejournals.org

Characterization of Force Deflection Properties for Vehicular Bumper-to-Bumper Interactions

Enrique Bonugli, Jeffrey Wirth, James Funk, Joseph Cormier, Herbert Guzman, Lisa Gwin, and Mark Freund
Biodynamic Research Corp.

ABSTRACT

This is the complete manuscript and replacement for SAE paper 2014-01-0482, which has been retracted due to incomplete content.

This paper reports on 76 quasi-static tests conducted to investigate the behavior of road vehicle bumper systems. The tests are a quasi-static replication of real world low speed collisions. The tests represented front to rear impacts between various vehicles. Force and deflection were captured in order to quantify the stiffness characteristics of the bumper-to-bumper system.

A specialized test apparatus was constructed to position and load bumper systems into each other. The purpose was to replicate or exceed damage that occurred in actual collisions. The fixture is capable of positioning the bumpers in various orientations and generates forces up to 50 kips. Various bumper-to-bumper alignments were tested including full overlap, lateral offset, and override/underride configurations. Force and displacement were recorded and the data was analyzed to develop system stiffness and crush parameters. These parameters can be used in a collision-based model to calculate vehicle delta-v (ΔV) and acceleration. The simulation uses an impact mechanics-based numerical algorithm published by Scott [6]. The paper reports on the test results of various combinations of vehicle categories. Vehicle type includes passenger, light transport and heavy vehicle bumper systems.

CITATION: Bonugli, E., Wirth, J., Funk, J., Cormier, J. et al., "Characterization of Force Deflection Properties for Vehicular Bumper-to-Bumper Interactions," *SAE Int. J. Trans. Safety* 2(2):2014, doi:10.4271/2014-01-1991.

INTRODUCTION

Assessing impact severity in low-speed collisions is often difficult using current accident reconstruction methods. In many cases vehicle specific crush stiffness data is not applicable or difficult to incorporate when dealing with vehicles that have little to no residual crush. Reconstructionists are routinely given sparse information regarding the accident vehicles which may or may not be available for inspection. Photographs, witness testimony and repair estimates are frequently the primary source of vehicle information regarding damage.

Traditional vehicle stiffness properties were first studied by Campbell [5] which defined the plastic deformation of vehicle structures in terms of equivalent barriers speed (EBS) and residual crush. The stiffness theory was further developed and uses what are currently known as stiffness coefficients. Campbell also described a non-zero intercept term that took into account the initial energy absorbed with no residual crush. The theory allows calculation of damage energy which can be used in conjunction with conservation of momentum and conservation of energy to determine the ΔV of the vehicles. However, the stiffness coefficients and intercept have limited application in low-speed impacts with minimal residual damage.

Strother et al. examined the use of deformation energy as an accident reconstruction tool to determine vehicle dynamics for a specific crash [10]. The method required vehicle specific crash data to establish deformation energy estimates. Various force models including the constant force, force saturation, and bilinear crush force model were explored. He stated the need for additional testing to supplement the low energy level data. He cautioned that the use of 30 to 35 mph barrier test data to estimate low speed collision could yield unrealistic stiffness estimates.

Another approach has been called the Momentum-Energy-Restitution (MER) method. This method is based on rigid body impact mechanics and uses impulse, conservation of momentum, conservation of energy and restitution to determine the ΔV of the vehicles in a low-speed crash [2,3,7].

In order to estimate the ΔV for a vehicle in a specific crash the MER method requires a value for the coefficient of restitution (ε) and an estimate of the energy absorbed by each vehicle during the crash. An analysis of a low-speed crash with the MER method provides a ΔV for the crash but does not provide the acceleration vs. time information for the vehicles during the crash.

A third approach is to treat the vehicles as rigid structures and model the bumpers as a spring/dashpot systems and then solve the governing differential equations with the appropriate initial conditions [2,7,12]. The solution gives the accelerations of both vehicles during the crash. In order to simulate a specific crash with a spring/dashpot model the appropriate stiffness and damping coefficients must be used.

Happer et al. [6] described a method for using the IIHS low speed crash test reports to establish an upper limit for crash severity. A comparison of damaged components between the test vehicle and the vehicle being investigated is made. If lesser damage is demonstrated on the vehicle being investigated when compared to the test vehicle then the closing velocity for the test can be used as an upper limit BEV for the subject vehicle. The BEV can in turn be used in the Carpenter [3] single-degree-of-freedom (SDOF) MER method, once b1 values have been determined. This method is useful when IIHS tests are available for a particular vehicle.

Scott developed a numerical collision model to simulate low-speed collinear vehicle-to-vehicle impacts. In the analysis the impact force was directly related to the physical properties of the bumpers that were involved in the crash [8,9]. The approach allows the crash severity of a low-speed crash involving specific vehicles to be estimated, including the crash pulse. This approach takes into account the variability of the force-deformation characteristics of the bumper systems. A numerical simulation is performed which satisfies Newton's Second Law at discrete time increments The structural characteristics of both vehicles' bumpers are combined and input as a system Impact Force-Deformation (IF-D) function. The deformation is the sum of the deformation of the two bumpers involved in the crash (i.e. mutual crush). The IF-D function can be a theoretical curve, or be based on measured force-deflection data for specific bumpers. Tests were conducted to measure IF-D curves which were then used in the analysis to determine the ΔV and the acceleration vs. time information for vehicles involved in crashes.

Validation of the quasi-static bumper loading method described in this paper has been conducted by Scott et al. A series of matching quasi-static and dynamic tests were performed and compared. The study concluded that quasi-static force deflection measurement can be used to reconstruct and quantify the vehicle dynamics in low speed bumper-to-bumper collisions.

This retrospective study provides a large number of force-deformation curves taken from tests covering a wide range of bumper systems. The testing is grouped into categories and summarized as linear IF-D functions. These functions could be used for the calculation of vehicle delta-v and acceleration in low-speed collisions when specific test data is not available. In that case the delta-v and acceleration are calculated in an analysis of the collision using a model based on Newton's Laws of Motion developed by Scott et al. The IF-D function characterizes the vehicle interaction.

METHOD

General

Bumper-to-bumper interactions were simulated using a test fixture developed to quasi-statically load two bumper systems as described by Scott [8,9]. The working model assumes each of the vehicles involved in the collision to be a rigid body with the exception of the interacting bumper and vehicle components. Many of the tests conducted were designed and modeled based on a real world low speed collision and were used to analyze the crash mechanics for that specific crash configuration. The bumper components were aligned using information available to the reconstructionist for the particular crash being investigated. Information available to the reconstructionist often included scene photographs, photographs of one or both vehicles involved in the crash, witness testimony, repair estimates, accident reports, and/or appraisal reports. For example, in some cases the front license plate or license plate fastener of the striking vehicle created an imprint onto the rear bumper cover of the struck vehicle. This physical evidence was used to align the bumper at the point of initial contact. Exemplar vehicles were procured for each bumper system in order to obtain external bumper cover and bumper reinforcement bar heights. In some instances bumper dive measurements due to heavy braking were also documented to ensure proper vertical bumper alignment.

The interacting bumpers are treated as a one system and therefore produce the stiffness characteristics for the system as a whole. The exemplar test components were fixed to the test apparatus rigidly and in a substantially similar mounting configuration when compared to their respective vehicles including all relevant bumper brackets. All tests were conducted using original equipment manufacturer (OEM) parts and brackets.

A total of 85 quasi-static force deflection bumper tests were reviewed. The bumper tests were sorted and grouped in a variety of category permutations for comparative analysis. Nine of the 85 did not form a significant category grouping and were not used in the analysis.

Each force deflection test consisted of two general phases, a compression phase and rebound phase. The front bumper system of one vehicle and the rear bumper system of another were compressed together in order replicate and/or exceed the damage seen on the vehicles being investigated. Only compression phases were comparatively analyzed for this study.

Test Apparatus

The test fixture is comprised of one fixed and one moveable steel plate as shown in Figure 1. Each bumper system is mounted to one of the steel plates. The moveable plate is guided along two tracks on roller bearings and is powered by two 4 inch diameter hydraulic cylinders operating at 2400psi.

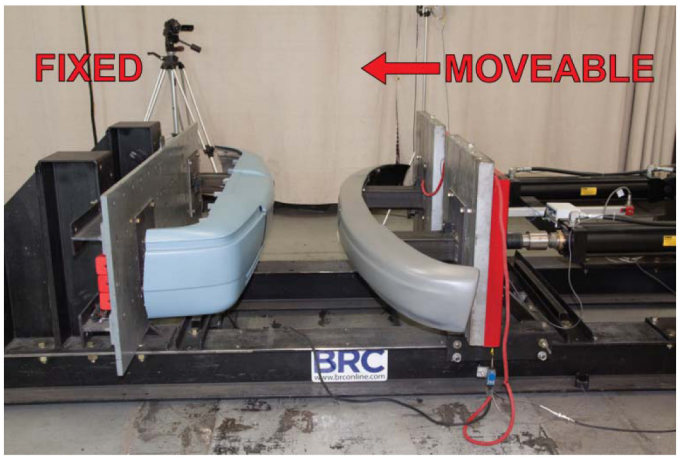

Figure 1. Photograph of the test apparatus designed to mount two bumper systems for a quasi-static compression test.

Override/underride configurations were tested in addition to the bumper-to-bumper interactions. The test fixture was modified by removing the fixed steel plate from the I-beam track. An exemplar vehicle, in its entirety, is then rigidly anchored to the fixture and ground as shown in Figure 2. In this configuration the suspension of the vehicle was allowed to respond normally in the vertical direction.

Figure 2. Photograph of the test apparatus modified for an override/underride condition. The fixed steel plate has been removed and a whole vehicle is rigidly anchored to the ground and fixture.

Instrumentation

The test machine was instrumented with two force transducers (1210AO-25k, Interface, Inc.) and a displacement transducer (Temposonics, E-Series, MTS, Inc.). The data acquisition system consisted of a 16-channel board (PCIMIO16E2, NI, Inc.) inside a Dell® workstation connected to a 3-channel bridge conditioner and amplifier system (136-1DC, Endevco, Inc.).

Documentation

All tests were documented using real-time digital video. The video cameras were synchronized in time with the force displacement data. Digital still photography was used to document the pre- and post-test condition of the bumper components. Comparative photographs were taken at similar angles and focal distances as the photographs of the vehicles being investigated.

Test Categories

Each test was categorized by vehicle type, vertical bumper alignment, horizontal bumper alignment, and whether or not the struck vehicle was equipped with a trailer hitch ball mount. The vehicle type was defined by the vehicle the bumper system originated from. The categories chosen were cars, which included passenger vehicles such as two or four door sedans and coupes, light transport vehicles (LTV's) including pickups, sport utility vehicles (SUV), and minivans, and heavy vehicles which included all commercial vehicles with a GVRW of 10,000 lbs or greater. For each test there was a striking and struck vehicle. Table 1 lists the test categories and the number of tests in each category.

Table 1. Test categories organized by vehicle type, vertical and horizontal alignment.

Vehicle Type	Vehicle Type	Alignment		Number
Striking Vehicle	Struck Vehicle	Vertical	Horizontal	of Tests
Car	Car	Bumper-to-Bumper	Full Overlap (> 50%)	18
LTV	LTV	Bumper-to-Bumper	Full Overlap (> 50%)	6
Car	LTV	Bumper-to-Bumper	Full Overlap (> 50%)	8
LTV	Car	Bumper-to-Bumper	Full Overlap (> 50%)	8
Heavy Veh.	Car/LTV	Bumper-to-Bumper	Full Overlap (> 50%)	5
All	All	Bumper-to-Trailer Hitch	Focal	8
All	All	Override/ Underride	All	13
All	All	Bumper-to-Bumper	Offset (< 50%)	10

RESULTS

Car-to-Car (CC), Full Vertical Overlap, Full Horizontal Overlap

The car-to-car, full overlap category included a total of 18 tests as shown in Figure 3. Manufacturers represented within this category were General Motors, Ford, Chrysler, Honda, Toyota, Suzuki, Mercedes, Mitsubishi, Hyundai, Jaguar, Volkswagen, Nissan and Volvo. A linear best fit slope for each test was

determined based on a zero y-intercept to peak force criterion. In many cases, the peak force may represents a global maximum rather than the force at peak deformation as shown in Figure 4. The maximum values located within the compression phase of a force deformation test often represented the collapse of a bumper component. The overall slope of the compression phase is the bumper system stiffness measured in pounds (force) per foot. The numerical average and one standard deviation of the bumper stiffness values were then used to create a bumper stiffness corridor. The average stiffness for this category was 29,591 lbf/ft with a standard deviation of 10,524 lbf/ft.

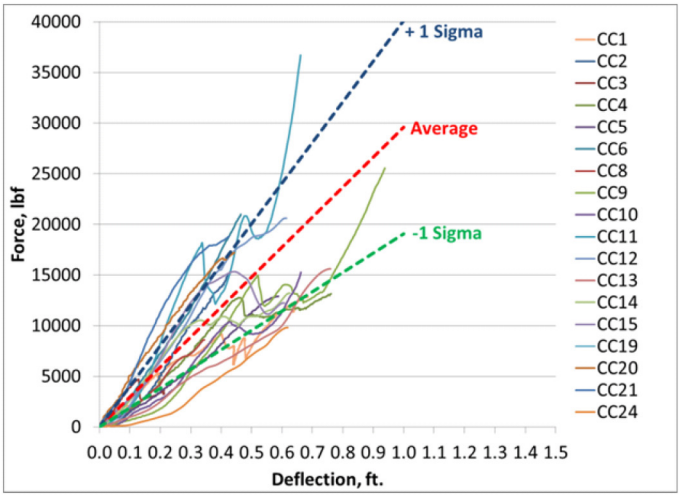

Figure 3. Force vs. deflection plot for the car-to-car full overlap tests. The average slope and standard deviation are overlaid on the test data.

The test shown below in Figure 4 is an example of a force deflection plot in which the front bumper system (striking vehicle) collapsed and could no longer support the compressive forces. In this case, the left bumper bracket and front reinforcement bar were compromised. The stiffness for this test was determined from the peak force rather than the peak deflection to better represent the resistance prior to collapse. The average slope would have been underestimated had the peak deflection been used as a stiffness determinant.

Two-thirds (12 of 18) of the tests in this category had a bumper reinforcement bar or bumper brackets that collapsed. A list of damaged components for these tests is detailed in Table 2. The average force for bumper reinforcement bar collapse was 12,800 lbf. Of the twelve tests that included bumper bar collapse, nine were front bumper systems. It was postulated that the front bumper systems for road vehicles are softer than rear bumper system because of the airbag system. The front bumper systems are possibly tuned with the deployment sequence of the vehicle. It was also observed that bumpers constructed from aluminum had a tendency to be stiffer than any other material tested.

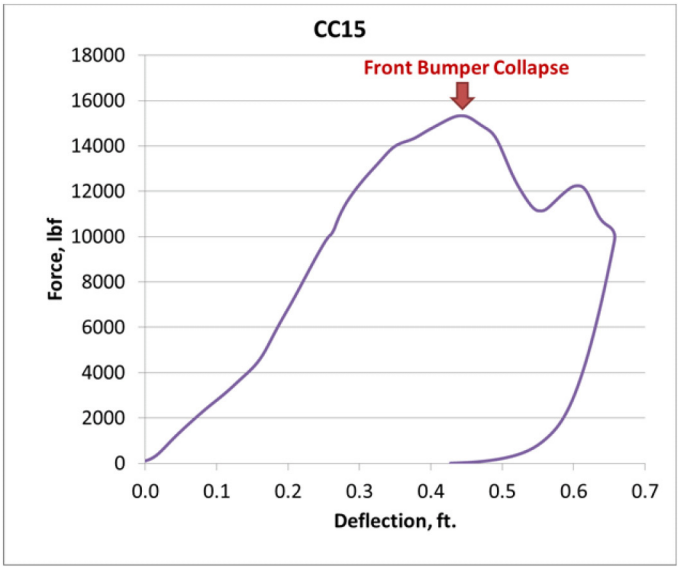

Figure 4. Force vs. deflection plot for test CC15 including the compression and rebound phase. The front bumper system permanently deforms at approximately 15,300 lbf.

Table 2. List of test components that permanently yielded in the car-to-car full overlap category.

Test I.D.	Material Type	Yield Force (lbf)	Description of Damaged Components
CC2	Steel	15300	Scion brackets permenantly deform
CC3	Fiberglass Composite	4637	Buick bumper reinforcement bar collapsed
CC4	Steel	12749	Acura bumper reinforcement bar collapsed
CC5	Steel	12863	Hyundai bumper reinforcement bar collapsed
CC8	PE	7000	Impala honeycomb energy absorber deformed
CC9	Steel	15000	Malibu bumper reinforcement bar collapsed
CC10	Steel	10300	Mitsubishi bumper reinforcement bar collapsed
CC11	Steel	17557	Toyota bumper reinforcement bar collapsed
CC13	Steel	15600	Ford bumper reinforcement bar collapsed
CC14	PE	10300	Pontiac bumper brackets and rebar collapsed
CC15	Fiberglass Composite	15168	Suzuki bumper reinforcement bar collapsed
CC21	Steel	17900	Honda bumper reinforcement bar collapsed

LTV-to-LTV (LL), Full Vertical Overlap, Full Horizontal Overlap

The LTV-to-LTV, full overlap category included a total of 6 tests as shown in Figure 5. Manufacturers included Chrysler, Ford, General Motors and Honda. The average stiffness for this category was 32,145 lbf/ft with a standard deviation of 11,387 lbf/ft.

The bumper construction and mounting differs between pickups and sedans. Pick-ups tend to lack bumper covers and energy absorbers. Additionally, the mounting structure consisted of brackets that are directly fastened to a box frame. Because of these differences in design, component yielding occurred within the compliance of the brackets. In some tests the rear bumper pitched instead of causing the bumper reinforcement bar to permanently deform. In other cases the bumper may not collapse but rather deform through indentation of the bumper fascia.

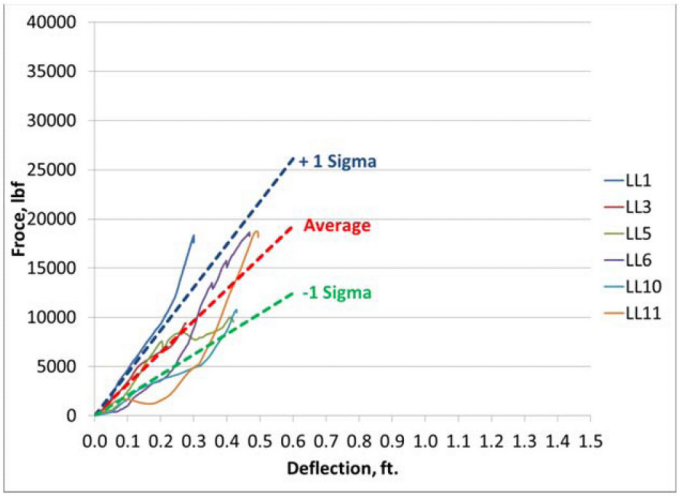

Figure 5. Force vs. deflection plot for the LTV-to-LTV full overlap tests. The average slope and standard deviation are overlaid on the test data.

Car-to-LTV (CL), Full Vertical Overlap, Full Horizontal Overlap

The car-to-LTV, full overlap category included a total of 8 tests as shown in Figure 6. Manufacturers included Ford, General Motors, Toyota, Isuzu and Honda. The average stiffness for this category was 28,296 lbf/ft with a standard deviation of 11,608 lbf/ft.

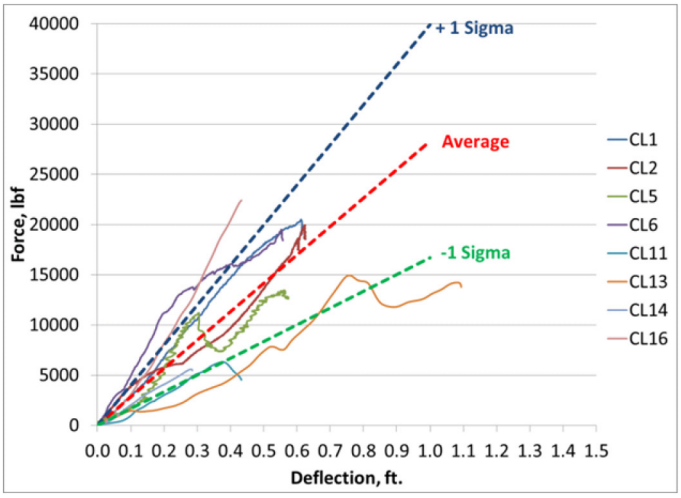

Figure 6. Force vs. deflection plot for the car-to-LTV full overlap tests. The average slope and standard deviation are overlaid on the test data.

This category had similar damage results when compared to the LTV-to-LTV category. This is in part due to the fact that the rear bumper systems are mostly pick-up bumpers. Yielding occurred when the rear bumper system rotated rather than plastically deforming. Three of the eight tests (CL1, CL2, and CL6) involved the front bumper system of a Ford Taurus. The Ford Taurus front bumper was noted as being relatively stiff and did not permanently deform. All three Ford Taurus tests resulted in similar stiffness slopes near the upper limit of the corridor.

LTV-to-Car (LC), Full Vertical Overlap, Full Horizontal Overlap

The LTV-to-car, full overlap category included a total of 8 tests as shown in Figure 7. Manufacturers included Ford, General Motors, Toyota, Isuzu and Honda. The average stiffness for this category was 29,245 lbf/ft with a standard deviation of 13,446 lbf/ft.

Five of the eight tests included a bumper system that collapsed, all of which were front bumpers. A majority of these front bumpers were from sport utility and minivan vehicles that closely resemble the construction of sedans. Two of the five bumpers were constructed from a fiberglass composite material. The average force for bumper reinforcement collapse for the five tests was 9,786 lbf.

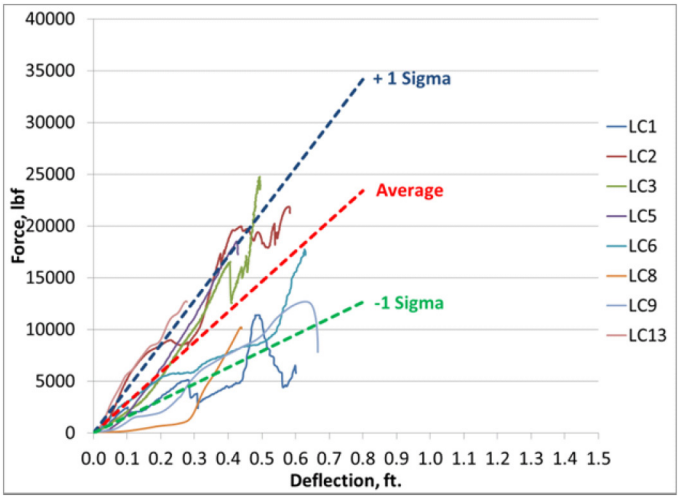

Figure 7. Force vs. deflection plot for the LTV-to-car full overlap tests. The average slope and standard deviation are overlaid on the test data.

Heavy Vehicle-To-Car/LTV (HC) (HL), Full Vertical Overlap, Full Horizontal Overlap

The heavy vehicle-to-car/LTV, full overlap category included a total of 5 tests as shown in Figure 8. Manufacturers included Ford, General Motors, Toyota, Peterbilt, International, Freightliner and Honda. The average stiffness for this category was 51,799 lbf/ft with a standard deviation of 29,699 lbf/.

In general, the heavy vehicle front bumper systems were stiffer than their car and LTV counterparts. Tests HC2 and HC4 were Peterbilt front bumpers and followed a distinctly similar force deflection characteristic. Both of these tests involved subject vehicles in which the struck car was left with only bumper fastener (bolt) impressions onto the rear bumper covers. This allowed for precise alignment of the bumpers at the time of impact. Preliminary tests were first conducted to create the bolt

impression onto the bumper covers before proceeding with the tests shown in Figure 8. The subsequent tests were then performed with the intent of grossly exceeding the damage documented on the subject vehicle to present a worst case scenario. Tests HC3 and HC4 followed a different pattern in both stiffness and damage. The bumper systems of the struck vehicles were comparatively less stiff than the heavy vehicle front bumpers and deformed to a greater extent. This created a large variation in the standard deviation for this category. It should be noted that in all five tests the heavy vehicle bumper fascia's plastically deformed. The stiffness of the front bumper system was generated from the interaction with the box frame and underlying bumper brackets rather than the bumper fascia which were all constructed from a thin gauge metal.

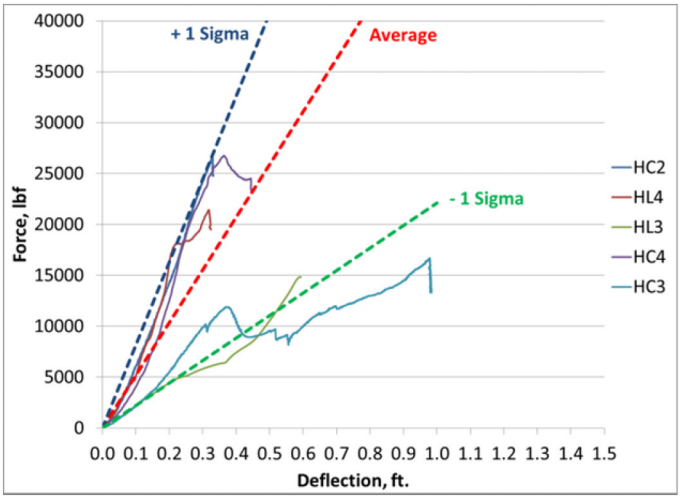

Figure 8. Force vs. deflection plot for the heavy vehicle-to-car/LTV full overlap tests. The average slope and standard deviation are overlaid on the test data.

All Car/LTV-to-Trailer Hitch

The car/LTV-to-trailer hitch, full overlap category included a total of 8 tests as shown in Figure 9. Manufacturers included Ford, General Motors, Toyota, Honda, and Nissan. The average stiffness for this category was 24,052 lbf/ft with a standard deviation of 4,163 lbf/ft.

All tests were conducted with the intent of collapsing the front bumper reinforcement bars. Trailer hitch ball mount collisions are a common crash type. They often lead to a distinct focal damage pattern ideal for aligning the vehicles at impact as shown in Figure 10. No test exceeded a peak force of 11,200 lbf. The average force for bumper collapse was 8,323 lbf. Test TH5 was the only test that did not involve a ball mount and only included the receiver box tubing although the data followed the same pattern as the remaining 7 tests. Ideally a bi-phasic slope would be used in the simulation to calculate ΔV and acceleration. The linearity of the average slope would tend to over predict the calculated values.

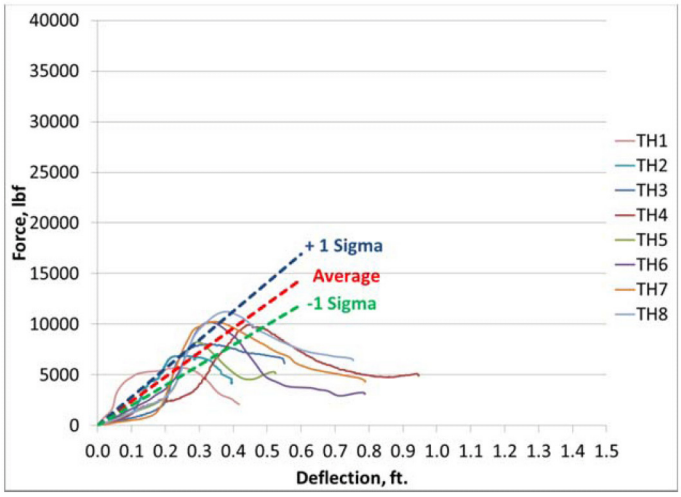

Figure 9. Force vs. deflection plot for all car/LTV-to-trailer hitch tests. The average slope and standard deviation are overlaid on the test data.

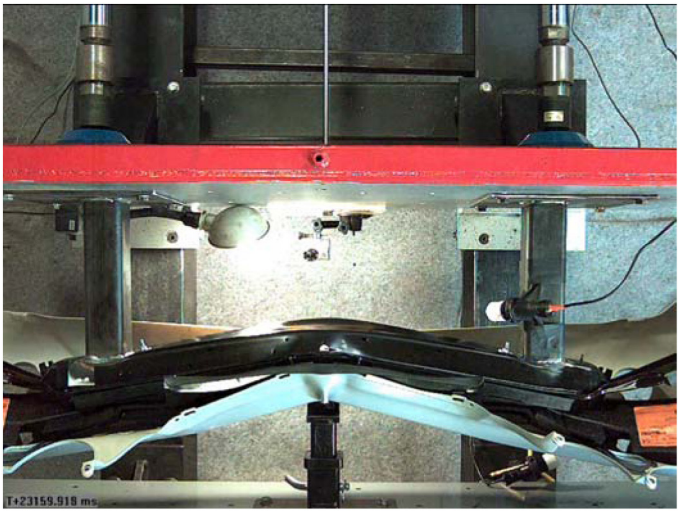

Figure 10. Overhead view of a trailer hitch equipped with a ball mount intruding into the front bumper system in test TH3 at maximum compression.

All Override/Underride

The Override/Underride category included a total of 14 tests as shown in Figure 11. Manufacturers represented within this category were General Motors, Ford, Lexus, Saturn, Hyundai, Hino, Chrysler, Nissan, Sterling and Toyota. The average stiffness for this category was 7,089 lbf/ft with a standard deviation of 3,764 lbf/ft.

During the tests the bumpers engaged and usually then slid over one another resulting in damage to components including the hood, grill, headlights, radiator support, truck lid, body panels, bumper and bumper covers. As the stiff structures were generally not damaged during the testing, the average stiffness is much lower than the other categories. There was a large variation in the vehicles tested, which included cars and LTV's. This may explain the relatively large standard deviation.

Struble et al. [11] characterized the override/underride crash condition by analyzing a series of staged flat barrier NCAP frontal crash tests referred to as the Volpe Tests. The load cell barrier data was used to determine the crush energy distribution of the structure above and below the top of the front bumper structures. They concluded that in those tests the upper structures absorbed only 10 to 29 percent of total crush energy. Although validation testing has not been conducted for the quasi-static override/underride test condition the average stiffness value was approximately 25 percent of the average car/LTV-to-car/LTV stiffness values. This test condition is an area of future research for the authors.

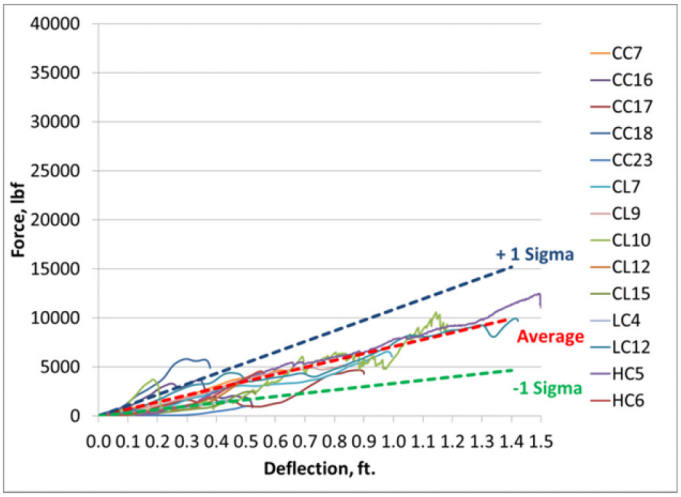

Figure 11. Force vs. deflection plot for all vehicle override/underride tests. The average slope and standard deviation are overlaid on the test data.

All Offset Horizontal Overlap, Full Vertical Overlap

The offset horizontal, full vertical overlap category included a total of 10 tests as shown in Figure 12. Manufacturers represented within this category were General Motors, Ford, Lexus, Infiniti, Great Dane and Toyota. The average stiffness for this category was 27,577 lbf/ft with a standard deviation of 19,964 lbf/ft.

All the tests resulted in damage to bumpers and bumper brackets, one test had damage to a rear body panel. While the average stiffness is similar to the other categories, the deviation is unusually large. This is due in part to the large range of the offset used, which varied from about a 45% overlap to a nearly corner-to-corner test. Also, there was a large variation in the vehicles tested, which included cars, LTV's and a trailer equipped with an ICC bumper. This large variety was necessitated by the limited number of offset tests that have been conducted. More testing may allow further differentiation of this category, and more limited corridors for the stiffness value.

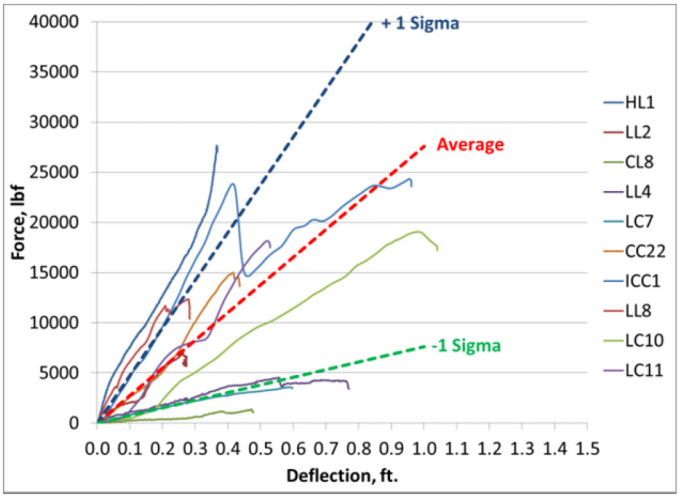

Figure 12. Force vs. deflection plot for all vehicle horizontal offset tests. The average slope and standard deviation are overlaid on the test data.

Case Study

A specific crash was reviewed in which a force deflection curve had already been generated for a reconstruction (CC9). This was a low-speed collision involving a 2001 Volvo V70 as the striking vehicle and a 2005 Chevrolet Malibu Maxx as the struck vehicle. Photographs and repair estimates for both vehicles were provided to the reconstructionist. The repair estimate for the Volvo stated the need to replace the front bumper license plate bracket while the repair estimate for the Chevrolet stated the need to replace the rear bumper cover. Damage to both vehicles was limited to the bumper systems as the interacting vehicle structures. An imprint of a license plate bracket onto the rear bumper cover of the struck vehicle was used to align the bumpers for the test. Bumper height measurements were obtained to confirm the bumper alignment. The car-to-car full overlap singular slope stiffness values reported in this paper were then used to numerically compute vehicle velocity and acceleration. The numerical algorithm applied to simulate the crash is located in the Appendix. These results were then compared to the multi slope stiffness curves (best fit) generated for the specific force deflection data for test CC9. The low-speed numerical crash simulation was modeled and executed in Matlab 7.14 (Mathworks, Inc.).

Figure 13 shows the extent of damage to the Volvo. The lower aspect of the license plate bracket is fractured and front bumper cover appears undamaged. The Volvo was not available for inspection by the reconstructionist. The driver of the Volvo stated that he was at a stop light behind the Chevrolet when his foot slipped off the brake and his car rolled into the car in front of him.

Figure 13. Photographs of the Volvo involved in the crash being investigated.

Figure 14 demonstrates the damage incurred to the Chevrolet. The rear bumper cover has areas of abrasion just right of center. The lower photograph in Figure 14 shows an outline of the license plate bracket imprinted onto the bumper cover that resulted from the collision. The Chevrolet was also not available for inspection.

The force deflection data produce in test CC9 was used to simulate the actual collision. Areas of inflection or local maxima often represent a point in which a component is compromised during the test. Figure 15 shows the force deflection data for test CC9. The peak force of 25,554 lbf occurred at 0.94 ft of deflection, however the rear bumper reinforcement bar for the Chevrolet collapsed at 15,000 lbf with 0.52 ft of deflection. The bumper yield point was used as an upper threshold for damage and signified the end of the simulation. The hysteresis or rebound phase of the force deflection curve could be used to model the separation phase of the collision. For simplicity a coefficient of restitution (ε) of 0.3 was used for the rebound phase of the crash simulation. Inclusion of the rebound phase is an area of future research. Using a range of restitutions could address this issue. Changing the restitution value will not affect the peak acceleration or peak force for the crash simulation, however it can alter the crash pulse duration and delta-v. In this case, the quasi-static test would ideally have been stopped once the Chevrolet reinforcement collapsed in order to capture the hysteresis at that point. Since the test was continued far beyond the bumper collapse, the restitution of the bumper system represents components being crushed beyond the point of collapse.

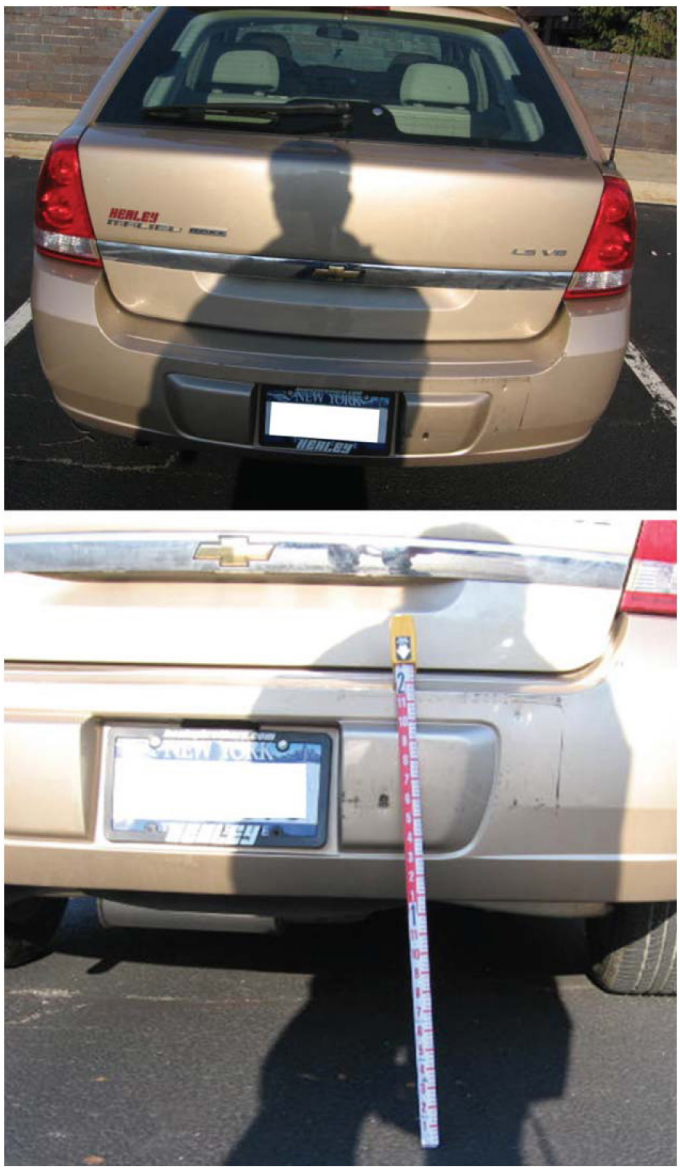

Figure 14. Photographs of the Chevrolet involved in the crash being investigated.

The best fit stiffness slope for the test data was divided into two phases. The first slope was measured from the test data to be 10,091 lbf/ft at 0.22 ft of deflection. The simulation continues from this point with a secondary slope of 42,200 lbf/ft until the bumper collapse at 0.52 ft of deflection. Maximum engagement is satisfied and the rebound phase begins until the forces reach zero.

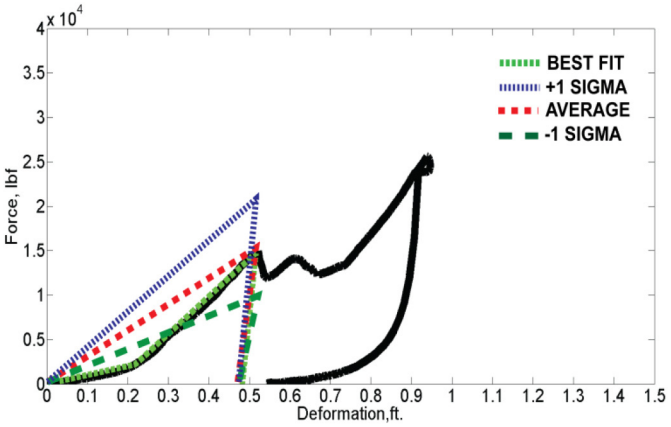

Figure 15. Force deflection data set for test CC9 overlaid with the best fit, average, minus one standard deviation and plus one standard deviation stiffness slopes. The stiffness corridors were obtained from the car-to-car full overlap data.

The iterative simulation completes the crash sequence and generates a velocity and acceleration time history based on the force deflection data. The area under the force deflection curve represents the work energy produced in the collision. The velocity time history shown in Figure 16 was calculated from the best fit stiffness slope simulation. The point of common velocity at 0.75 seconds is also the point of maximum engagement.

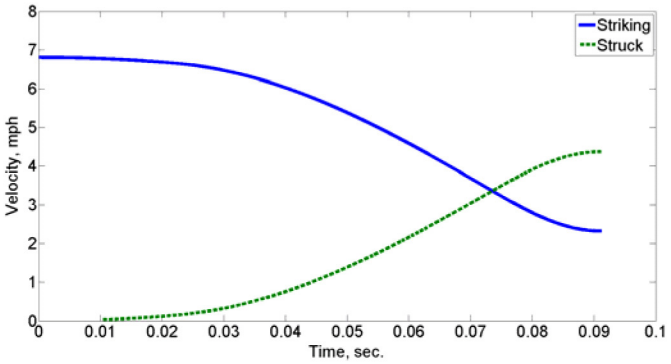

Figure 16. Velocity time history calculated from the crash simulation using the best fit slope data.

Next, the car-to-car full overlap stiffness corridors were then used as the stiffness input to execute the crash simulation. The average stiffness for this corridor was 29,591 lbf/ft with a standard deviation of 10,524 lbf/ft. The uniform slopes were overlaid with the best fit and test CC9 force deflection plot in Figure 15. The simulation was ended at 0.52 feet of deflection for each simulation. The acceleration time histories for the struck vehicle are plotted together in Figure 17 to compare peak values and crash duration. The average stiffness slope for this simulation produced an acceleration profile closest to the best fit data.

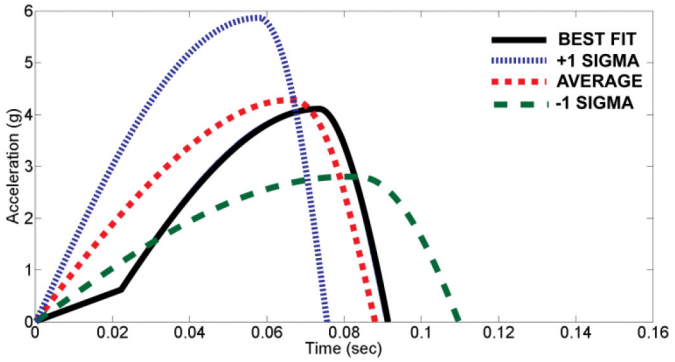

Figure 17. Acceleration time history plot of the struck vehicle for each crash simulation.

The pertinent output data for each simulation was summarized in Table 3. Change in velocity is often the most significant metric for crash severity used in accident reconstruction. The - 1 sigma corridor produced a ΔV within 5 percent of the best fit output. For this case study the +1 sigma overestimated the crash severity by nearly 40 percent. Overall the stiffness corridor would have captured the collision event by producing an upper and lower limit within a reasonable degree of accuracy.

In the event that test data is not available to the reconstructionist, an exemplar vehicle matchup, photogrammetry or three dimensional models can be used to estimate mutual crush. The estimation of crush can provide a metric to iterate the crash simulation based on the appropriate stiffness corridors reported in this paper.

Using a classic damage based crush analysis for the Volvo with vehicle specific A and B stiffness coefficients and uniform crush of 3 inches across the front of the Volvo yielded a BEV of 10.3 mph. Utilizing the conservation of momentum, the ΔV for the Chevrolet would be in excess of 10 mph. This demonstrates how the classic damage based analysis can over predict the vehicle ΔV's in low-speed collisions.

Table 3. Summary of results for the low-speed simulations completed for various stiffness slopes.

Method	Closure Velocity (mph)	Delta-V Struck Veh. (mph)	Peak Acceleration (g)	Delta-V % Error
Best Fit	6.8	4.4	4.1	-
Average	8.2	5.2	4.3	18
+1 Sigma	9.5	6.1	5.8	39
-1 Sigma	6.6	4.2	2.8	5

Residual Crush

The residual crush for each of the force deflection tests was measured and plotted with the corresponding peak deflection as shown in Figure 18. The relationship is fairly linear and indicates that the bumper systems rebound approximately 30 percent from maximum deflection.

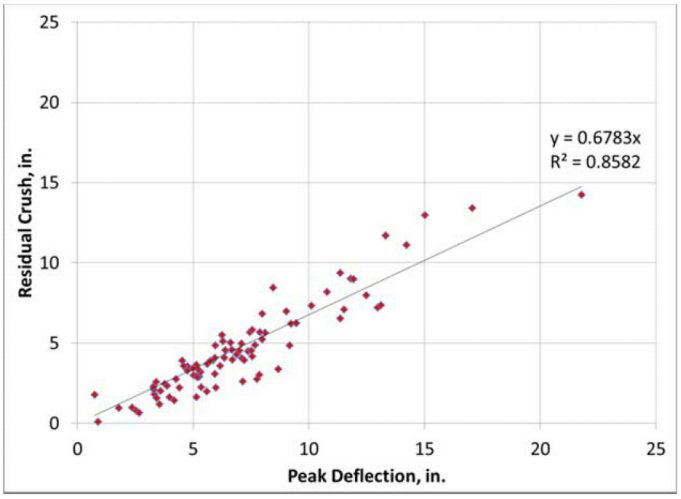

Figure 18. Residual crush for each of the force deflection tests performed.

SUMMARY/CONCLUSIONS

This paper has presented 76 quasi-static tests conducted on road vehicle bumper systems representing front to rear impacts between various vehicles. Force and deflection data for the tests was captured and plotted. These tests were conducted to obtain data to facilitate the reconstruction of various roadway crashes. In the absence of case specific testing, this large volume of test data can be used in a reconstruction. To better match specific impacts, categories were chosen representing combinations of various vehicle types common in roadway collisions. The stiffness characteristics of the bumper-to-bumper system was measured from each test and the average values for each category were determined. Table 4 gives the averages and standard deviations for the categories. The average stiffness values were similar for the various combinations of car and LTV impacts, perhaps reflecting similarity in general bumper system construction and impact response for passenger and light transport vehicles.

The average and standard deviation values create stiffness corridors as shown in Figures 6, 7, 8, 9 and 11-12. The corridors represent stiffness bounds that can be used in the calculation of collision parameters, such as ΔV and peak accelerations, using the numerical collision simulation describes by Scott [8] Mutual crush can be approximated through exemplar vehicle, three dimensional models or photogrammetry to determine peak deflection. This method serves as an additional tool for accident reconstruction when test data is limited or damage to the vehicles being investigated is not measureable.

Table 4. Average slopes for all test categories.

Category	Average Stiffness (lbf/ft)	Standard Deviation (lbf/ft)
Car-to-Car Full Overlap	29592	10524
LTV-to-LTV Full Overlap	32145	11387
Car-to-LTV Full Overlap	28296	11608
LTV-to-Car Full Overlap	29245	13446
Heavy Vehicle to LTV/Car Full Overlap	51799	29699
Trailer Hitch	24052	4163
All Override/Underride	7089	3764
All Offset	27577	19964

Further testing and analysis will allow finer differentiation of the vehicle categories and definition of the system stiffness characteristics.

REFERENCES

1. Bailey, M., Wong, B., and Lawrence, J., “Data and Methods for Estimating the Severity of Minor Impacts,” SAE Technical Paper 950352, 1995, doi:10.4271/950352.
2. Brach, R., “Modeling of Low-Speed, Front-to-Rear Vehicle Impacts,” SAE Technical Paper 2003-01-0491, 2003, doi:10.4271/2003-01-0491.
3. Carpenter, N. and Welcher, J., “Stiffness and Crush Energy Analysis for Vehicle Collision and its Relationship to Barrier Equivalent Velocity (BEV),” SAE Technical Paper 2001-01-0500, 2001, doi:10.4271/2001-01-0500.
4. Cipriani, A., Bayan, F., Woodhouse, M., Cornetto, A. et al., “Low Speed Collinear Impact Severity: A Comparison Between Full Scale Testing and Analytical Prediction Tools with Restitution Analysis,” SAE Technical Paper 2002-01-0540, 2002, doi:10.4271/2002 01 0540.
5. Campbell, K., “Energy Basis for Collision Severity,” SAE Technical Paper 740565, 1974, doi:10.4271/740565.
6. Happer, A., Hughes, M., Peck, M., and Boehme, S., “Practical Analysis Methodology for Low Speed Vehicle Collisions Involving Vehicles with Modern Bumper Systems,” SAE Technical Paper 2003-01-0492, 2003, doi:10.4271/2003-01-0492.
7. Ojalvo, I., Weber, B., Evensen, D., Szabo, T. et al., “Low Speed Car Impacts with Different Bumper Systems: Correlation of Analytical Model with Tests,” SAE Technical Paper 980365, 1998, doi:10.4271/980365.
8. Scott, W., Bain, C., Manoogian, S., Cormier, J. et al., “Simulation Model for Low-Speed Bumper-to-Bumper Crashes,” *SAE Int. J. Passeng. Cars - Mech. Syst.* 3(1):21-36, 2010, doi:10.4271/2010-01-0051.
9. Scott, W., Bonugli, E., Guzman, H., and Swartzendruber, D., “Reconstruction of Low-Speed Crashes using the Quasi-Static Force vs. Deformation Characteristics of the Bumpers Involved in the Crashes,” *SAE Int. J. Passeng. Cars - Mech. Syst.* 5(1):592-611, 2012, doi:10.4271/2012-01-0598.
10. Strother, C., Woolley, R., James, M., and Warner, C., “Crush Energy in Accident Reconstruction,” SAE Technical Paper 860371, 1986, doi:10.4271/860371.
11. Struble, D., Welsh, K., and Struble, J., “Crush Energy Assessment in Frontal Underride/Override Crashes,” SAE Technical Paper 2009-01-0105, 2009, doi:10.4271/2009-01-0105.
12. Thompson, R.W. and Romily, D.P. “Simulation of Bumpers During Low Speed Impacts”, Proceeding of the Canadian Multidisciplinary Road Safety Conference III. Saskatoon, Saskatchewan, Canada, 1993.

CONTACT INFORMATION

Enrique Bonugli
Biodynamic Research Corporation
5711University Heights Blvd., Suite 107
San Antonio, Texas 78249
Phone: (210) 691-0281
Fax: (210) 691-8823
ebonugli@brconline.com

ACKNOWLEDGMENTS

The authors acknowledge the work of BRC's Research Test Center who performed all of the force deflection tests.

APPENDIX

ALGORITHM FOR THE IMPACT SIMULATION MODEL BY SCOTT ET AL.

The numerical simulation starts at t=0 (j=1) with the vehicles in contact and the initial conditions required are vehicle speeds ($V_{1,1}$,$V_{2,1}$), and the center of mass positions ($X_{1,1}$,$X_{2,1}$) along the line the vehicles are traveling. Since the vehicles are in contact but not deformed the undeformed distance (UD) between the two centers of mass is

$$UD = X_{2,1} - X_{1,1}$$

At the first time position $A_{1,1} = A_{2,1}$=0, and the vehicles move forward through the first time step at their initial velocities and the velocities at the second time position (j=2) are the same as the initial conditions, $V_{1,1}$=$V_{1,2}$ and $V_{2,1}$= $V_{2,2}$. At the second time position the vehicles' center of mass positions are

$$X_{i,2} = X_{i,1} + V_{i,1}\,\Delta t \quad (i=1,2)$$

This movement of the centers of mass of each vehicle creates an overlap of the vehicles, and the deformation (D_j) at the second and following time positions (j=>2) is

$$D_j = UD - (X_{2,j} - X_{1,j})$$

The impact force $F_{i,j}$ that acts on each vehicle during the j^{th} time step (j>=2) is based on the input IF-D function and Newton's Third Law,

$$-F_{1,j} = F_{2,j} = \text{Function}\,(D_j)$$

The force $F_{i,j}$ (i=1,2) acts on the vehicles during the j^{th} time step where j>=2. Newton's Second Law is used to calculate the acceleration of each vehicle during the j^{th} time step,

$$A_{i,j} = F_{i,j} / M_i \qquad (i=1,2)$$

The impact forces accelerate the vehicles over the j^{th} time step. The time position is incremented, j = j+1, and the velocities at the new time position j are calculated,

$$V_{i,j} = V_{i,j-1} + A_{i,j-1}\,\Delta t \qquad (i=1,2)$$

The algorithm then checks to see if the vehicles have reached a common velocity. If the vehicles have reached a common velocity Function (D_j) is changed to represent the rebound phase of the input IF-D function. The simulation then calculates the vehicle center of mass positions at the new time position,

$$X_{i,j} = X_{i,j-1} + V_{i,j-1}\ \Delta t\ + \tfrac{1}{2}\, A_{i,j-1}\,\Delta t^2 \qquad (i=1,2)$$

The simulation then recalculates the variables and continues to move forward in time until $F_{i,j}$ (i=1,2) reaches zero and the crash is over.

Table 5. List of all test vehicles and alignement by category.

	Striking Vehicle			Struck Vehicle			Alignment				
							Vertical		Horizontal		
Test ID	Year	Make	Model	Year	Make	Model	Bumper-to-Bumper	Override/ Underride	Full Overlap (> 50%)	Offset (< 50%)	Focal
CC1	1999	Lincoln	Towncar	2001	Lincoln	Towncar	1	0	1	0	0
CC2	2006	Scion	xB	2007	Ford	Mustang	1	0	1	0	0
CC3	2006	Acura	TL	1993	Buick	Lesabre	1	0	1	0	0
CC4	2004	Acura	TSX	1999	Oldsmobile	Alero	1	0	1	0	0
CC5	2005	Hyundai	Elantra	2001	Saturn	LS1	1	0	1	0	0
CC6	2005	Toyota	Camry	2003	Jaguar	S-Type	1	0	1	0	0
CC7	2000	Saturn	SL2	2002	Hyundai	Sonata	0	1	1	0	0
CC8	2007	Chevrolet	Impala	1999	Honda	Civic	1	0	1	0	0
CC9	2001	Volvo	V70	2005	Chevrolet	Malibu Maxx	1	0	1	0	0
CC10	2004	Mitsubishi	Lancer	2005	Ford	Freestyle	1	0	1	0	0
CC11	2007	Toyota	Camry	2005	Mitsubishi	Galant	1	0	1	0	0
CC12	1993	Mercedes	300SE	1997	Chevrolet	Malibu	1	0	1	0	0
CC13	1995	Pontiac	Grand Prix	1995	Ford	Taurus	1	0	1	0	0
CC14	1999	Pontiac	Grand Am	2006	Chevrolet	Cobalt	1	0	1	0	0
CC15	2008	Suzuki	SX4	2006	Chrysler	300	1	0	1	0	0
CC16	2002	Chrysler	PT Cruiser	1995	Toyota	Camry	0	1	1	0	0
CC17	2001	Saturn	LS1	2000	Nissan	Maxima	0	1	1	0	0
CC18	2010	Toyota	Corolla	2007	Toyota	Camry	0	1	0	0	0
CC19	2008	Dodge	Avenger	2002	Jaguar	S-Type	1	0	1	0	0
CC20	2010	Honda	Accord	2000	Volkswagen	Beetle	1	0	1	0	0
CC21	2010	Honda	Accord	2000	Volkswagen	Beetle	1	0	1	0	0
CC22	2008	Ford	Focus	2007	Lexus	ES350	1	0	0	1	0
CC23	1997	Saturn	SL1	2009	Chevrolet	Cobalt	0	1	1	0	0
CC24	1997	Saturn	SL1	2009	Chevrolet	Cobalt	1	0	1	0	0
CL1	2004	Ford	Taurus	1998	Isuzu	Hombre	1	0	1	0	0
CL2	2004	Ford	Taurus	2005	Chevrolet	Expressvan	1	0	1	0	0
CL3	2004	Nissan	Sentra	2005	Hyundai	Tucson	1	0	0	1	1
CL4	2007	Mazda	3	2002	Jeep	Liberty	1	0	0	1	1
CL5	2006	Nissan	Sentra	2006	Honda	Odyssey	1	0	1	0	0
CL6	2008	Ford	Taurus	1982	Chevrolet	k10	1	0	1	0	0
CL7	2007	Toyota	Solara	2005	Toyota	Highlander	0	1	1	0	0
CL8	2003	Buick	Century	2008	Toyota	Rav4	1	0	0	1	0
CL9	2006	Hyundai	Elantra	2004	Nissan	Murano	0	1	0	1	0
CL10	2006	Ford	Crown Victoria	2006	Dodge	Durango	0	1	1	0	0
CL11	2002	Lexus	SC430	2001	Ford	Sport Trac	1	0	1	0	0
CL12	1996	Toyota	Camry	2007	Lexus	RX350	0	1	0	1	1
CL13	2007	Chevrolet	Impala	2000	Ford	Expedition	1	0	1	0	0
CL14	2011	Lexus	GS350	2005	Chevrolet	Silvarado 1500	1	0	1	0	0
CL15	2008	Hyundai	Accent	2009	Toyota	Tacoma	0	1	1	0	0
CL16	2008	Toyota	Corolla	1989	Ford	Ranger	1	0	1	0	0
HC1	2007	Freightliner	Columbia	2006	Scion	xA	1	0	1	0	1
HC2	2006	Peterbilt	379	2003	Buick	Century	1	0	1	0	0
HC3	2003	International	9400	1994	Toyota	Camry	1	0	1	0	0
HC4	2005	Peterbilt	389	1997	Acura	CL	1	0	1	0	0
HC5	2009	Hino	268	1995	Chevrolet	Cavalier	0	1	1	0	0
HC6	2002	Sterling	L9500	2004	Nissan	350z	0	1	1	0	0
HL1	2000	Cement	Truck	1996	Chevrolet	C1500	1	0	0	1	0
HL2	2009	Nissan	UD2000	2005	Ford	F250	1	0	1	0	1
HL3	2002	Freightliner	Columbia	2006	Ford	F250	1	0	1	0	0
HL4	2006	Chevrolet	C5500	2001	Ford	Explorer	1	0	1	0	0
ICC1	2002	Ford	F250	2007	Great Dane	ICC	1	0	0	1	0
LC1	1995	Dodge	Caravan	2005	Acura	RL	1	0	1	0	0
LC2	2003	Ford	Escape	2002	Honda	Civic	1	0	1	0	0
LC3	2005	Kia	Sedona	1991	Nissan	300zx	1	0	1	0	0
LC4	2006	Ford	Escape	2006	Chevrolet	Impala	0	1	0	1	0
LC5	2001	Oldsmobile	Silhouette	1998	Honda	Accord	1	0	1	0	0
LC6	2000	Chevrolet	Astro	2009	Mini	Cooper	1	0	1	0	0
LC7	2006	Ford	F150	2009	Infiniti	G37	1	0	0	1	0
LC8	2010	Jeep	Cherokee	2006	Ford	Freestyle	1	0	1	0	0
LC9	2006	Jeep	Commander	2003	Audi	A4	1	0	1	0	0
LC10	2003	Ford	Ranger	2006	ford	crown victoria	1	0	0	1	0
LC11	1997	Ford	Explorer	2006	Chevrolet	HHR	1	0	0	1	0
LC12	2007	Dodge	Ram 3500	2008	Nissan	Altima	0	1	0	1	0
LC13	1999	GMC	G3500	1999	Mercury	Grand Marquis	1	0	1	0	0
LL1	1988	GMC	C3500	2004	Honda	Pilot	1	0	1	0	0
LL2	1999	Ford	F150	2002	Toyota	Tacoma	1	0	0	1	0
LL3	2003	Ford	F250	2002	Chevrolet	Tahoe	1	0	1	0	0
LL4	2007	Chevrolet	Express Van	2003	Chevrolet	Avalanche	1	0	0	1	0
LL5	1993	Dodge	Grand Caravan	2000	Dodge	Durango	1	0	1	0	0
LL6	1999	Ford	F150	2008	Ford	F250	1	0	1	0	0
LL7	2006	Ford	F150	2004	Chevrolet	Trailblazer	1	0	0	1	1
LL8	2007	Ford	E150	2008	Chevrolet	Colorado	1	0	0	1	0
LL9	2002	Ford	E450	2003	GMC	Envoy	1	0	1	0	1
LL10	2003	Dodge	Ram 1500	2000	Dodge	Caravan	1	0	1	0	0
LL11	2008	Dodge	Sprinter	1994	Ford	Ranger	1	0	1	0	0
LL12	2002	Ford	E350	2005	Toyota	Tundra	1	0	1	0	1
LL13	2003	Ford	E350	2008	Chevrolet	Trailblazer	1	0	1	0	1
LL14	2003	Ford	E350	2008	Chevrolet	Trailblazer	1	0	1	0	1
TH1	1997	Ford	F150	1999	Trailer Hitch	Ball Mount	1	0	1	0	1
TH2	2007	Toyota	Camry	1999	Trailer Hitch	Ball Mount	1	0	1	0	1
TH3	2007	Toyota	Corolla	2012	Trailer Hitch	Ball Mount	1	0	0	0	1
TH4	2005	Chrysler	Sebring	2012	Trailer Hitch	Ball Mount	1	0	0	0	1
TH5	2006	Nissan	Sentra	2012	Trailer Hitch	Receiver	1	0	0	0	1
TH6	2009	Pontiac	Vibe	1998	Trailer Hitch	Ball Mount	1	0	1	0	1
TH7	1997	Honda	Prelude	1999	Trailer Hitch	Ball Mount	1	0	1	0	1
TH8	1998	Plymouth	Voyager	1999	Trailer Hitch	Ball Mount	1	0	1	0	1

FORCE (LBF) V DEFLECTION (FT) PLOTS FOR ALL TESTS

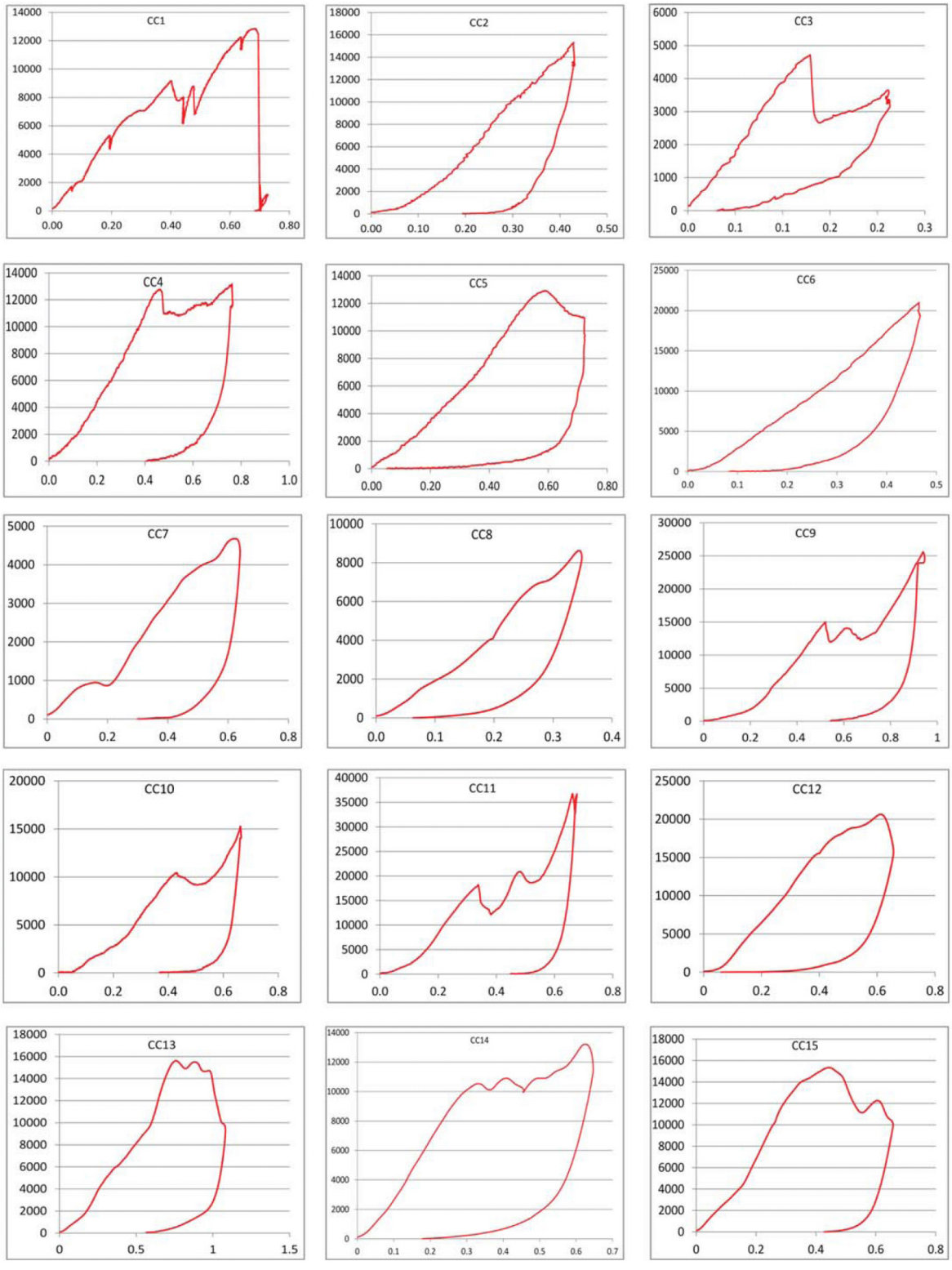

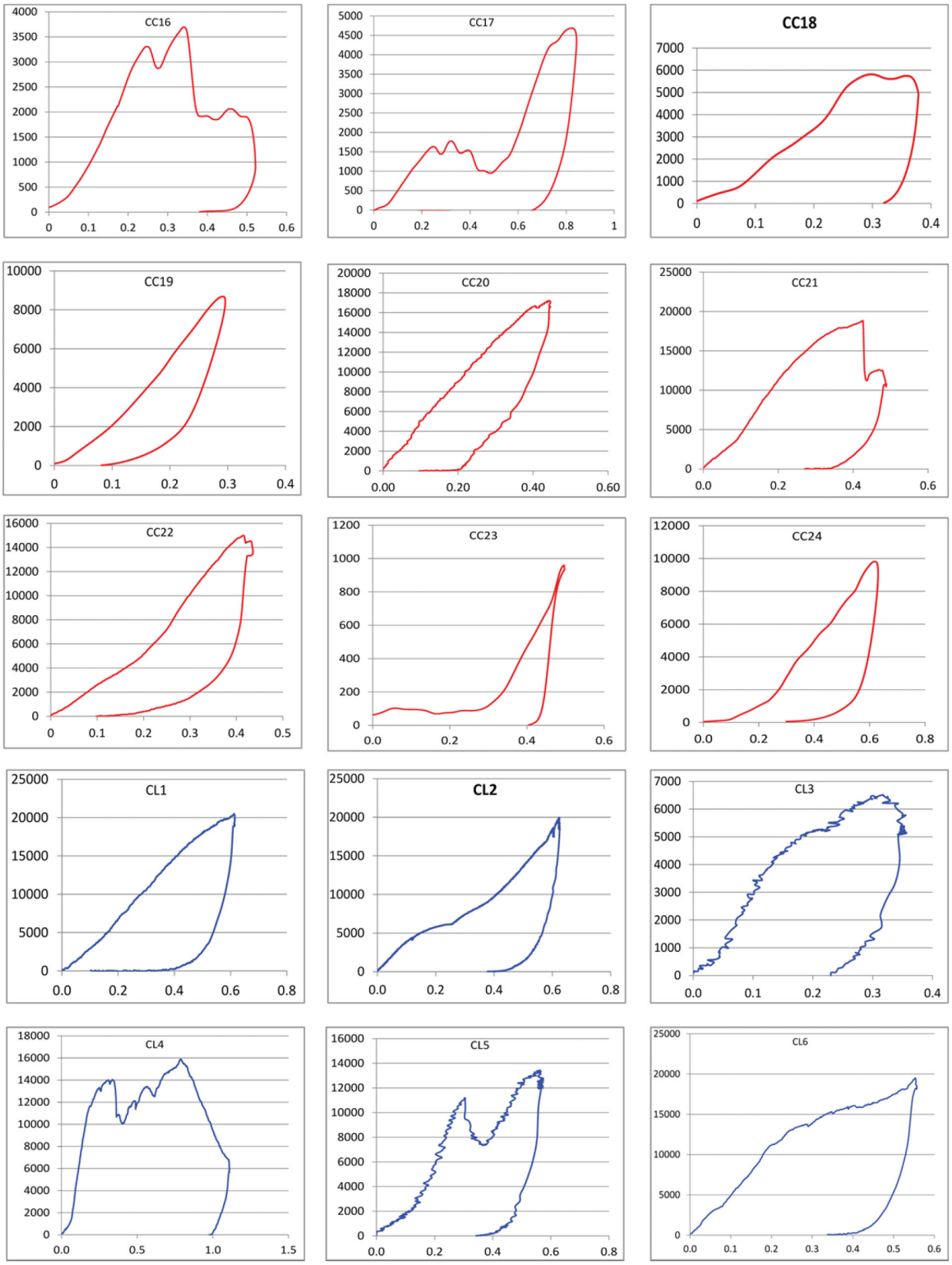
CC16
CC17
CC18
CC19
CC20
CC21
CC22
CC23
CC24
CL1
CL2
CL3
CL4
CL5
CL6

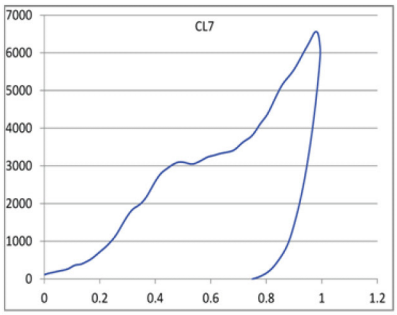
CL7
7000
6000
5000
4000
3000
2000
1000
0
0 0.2 0.4 0.6 0.8 1 1.2

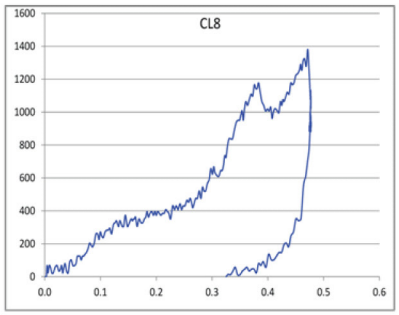
CL8
1600
1400
1200
1000
800
600
400
200
0
0.0 0.1 0.2 0.3 0.4 0.5 0.6

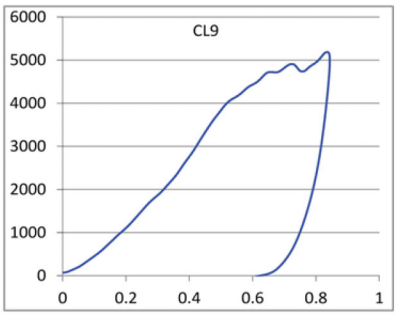
CL9
6000
5000
4000
3000
2000
1000
0
0 0.2 0.4 0.6 0.8 1

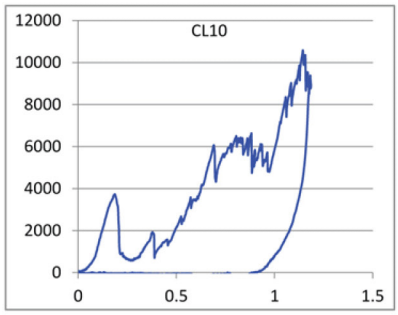
CL10
12000
10000
8000
6000
4000
2000
0
0 0.5 1 1.5

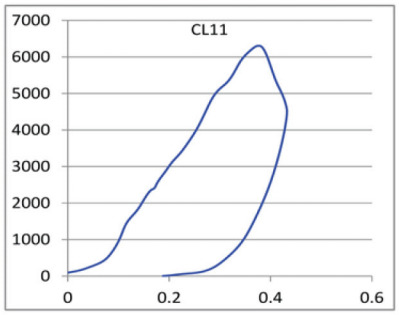
CL11
7000
6000
5000
4000
3000
2000
1000
0
0 0.2 0.4 0.6

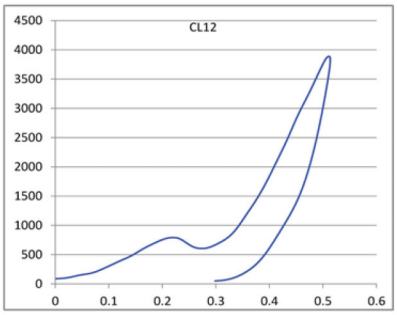
CL12
4500
4000
3500
3000
2500
2000
1500
1000
500
0
0 0.1 0.2 0.3 0.4 0.5 0.6

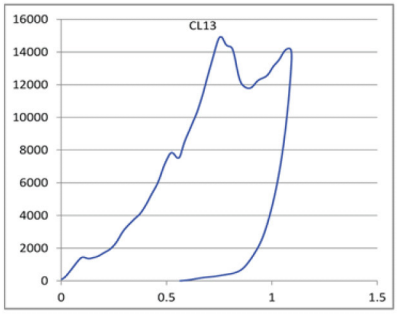
CL13
16000
14000
12000
10000
8000
6000
4000
2000
0
0 0.5 1 1.5

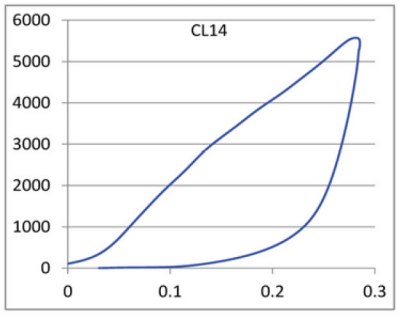
CL14
6000
5000
4000
3000
2000
1000
0
0 0.1 0.2 0.3

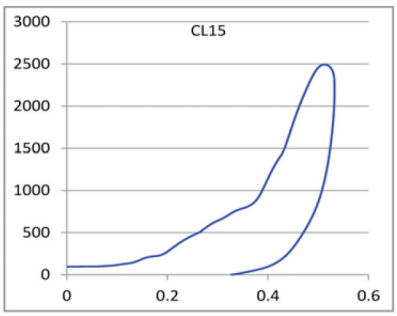
CL15
3000
2500
2000
1500
1000
500
0
0 0.2 0.4 0.6

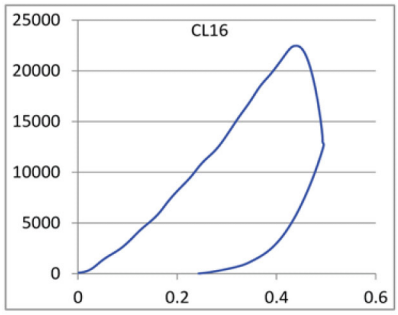
CL16
25000
20000
15000
10000
5000
0
0 0.2 0.4 0.6

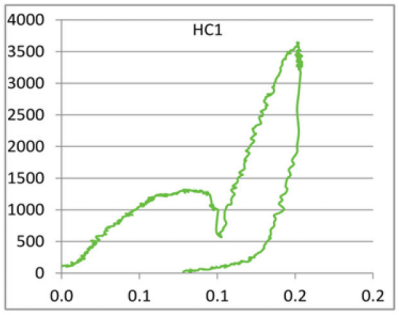
HC1
4000
3500
3000
2500
2000
1500
1000
500
0
0.0 0.1 0.1 0.2 0.2

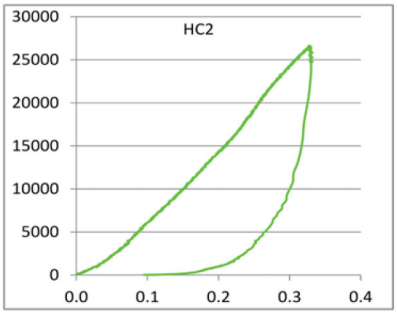
HC2
30000
25000
20000
15000
10000
5000
0
0.0 0.1 0.2 0.3 0.4

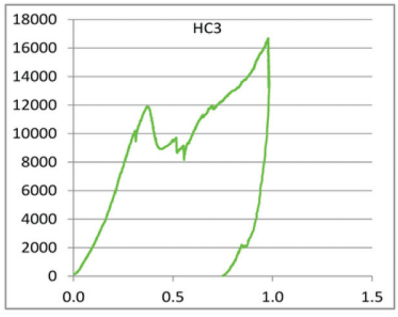
HC3
18000
16000
14000
12000
10000
8000
6000
4000
2000
0
0.0 0.5 1.0 1.5

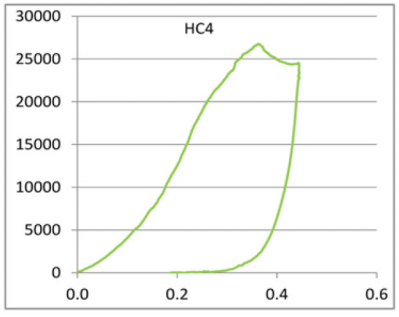
HC4
30000
25000
20000
15000
10000
5000
0
0.0 0.2 0.4 0.6

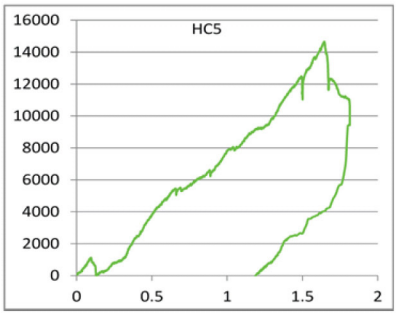
HC5
16000
14000
12000
10000
8000
6000
4000
2000
0
0 0.5 1 1.5 2

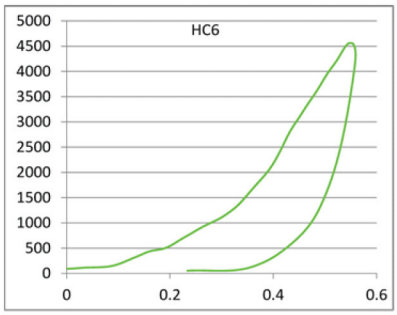
HC6
5000
4500
4000
3500
3000
2500
2000
1500
1000
500
0
0
0.2
0.4
0.6

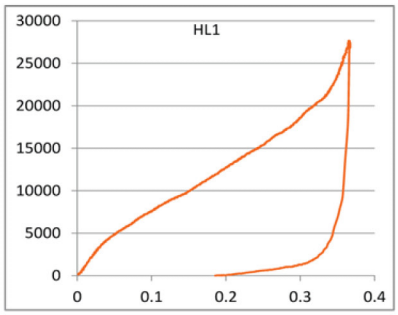
HL1
30000
25000
20000
15000
10000
5000
0
0
0.1
0.2
0.3
0.4

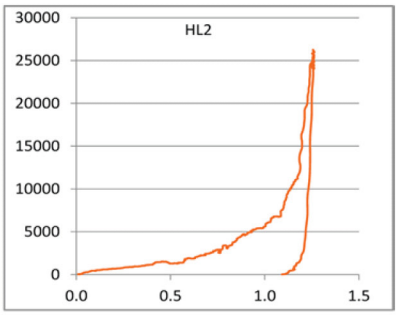
HL2
30000
25000
20000
15000
10000
5000
0
0.0
0.5
1.0
1.5

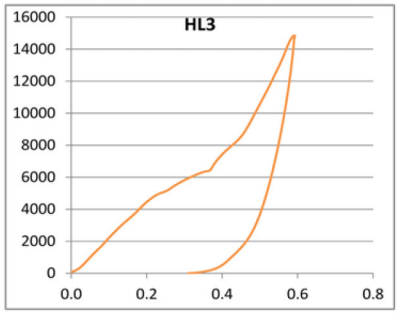
HL3
16000
14000
12000
10000
8000
6000
4000
2000
0
0.0
0.2
0.4
0.6
0.8

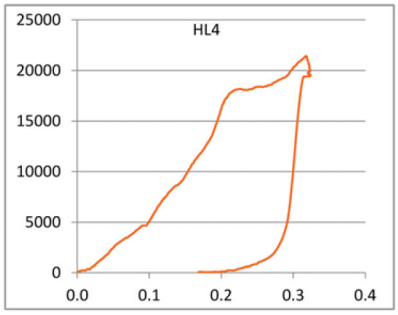
HL4
25000
20000
15000
10000
5000
0
0.0
0.1
0.2
0.3
0.4

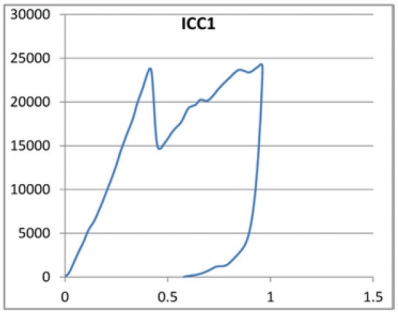
ICC1
30000
25000
20000
15000
10000
5000
0
0
0.5
1
1.5

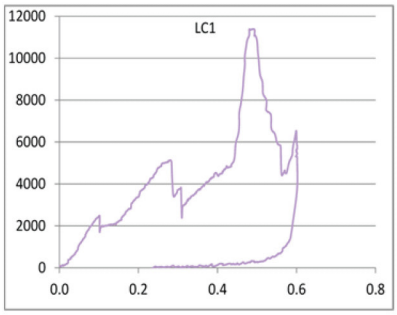
LC1
12000
10000
8000
6000
4000
2000
0
0.0
0.2
0.4
0.6
0.8

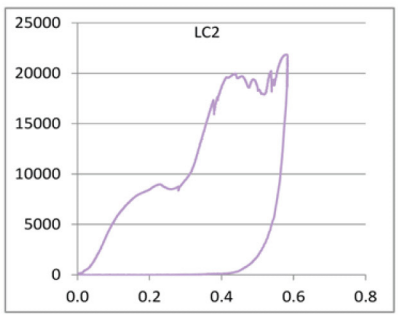
LC2
25000
20000
15000
10000
5000
0
0.0
0.2
0.4
0.6
0.8

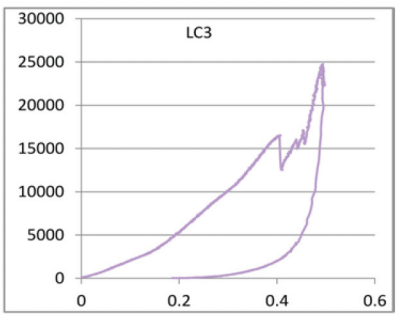
LC3
30000
25000
20000
15000
10000
5000
0
0
0.2
0.4
0.6

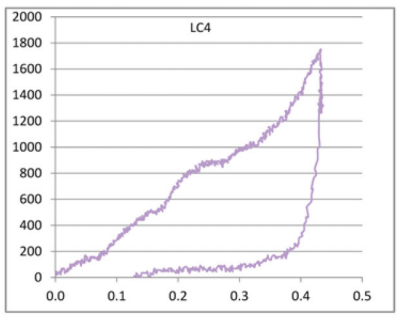
LC4
2000
1800
1600
1400
1200
1000
800
600
400
200
0
0.0
0.1
0.2
0.3
0.4
0.5

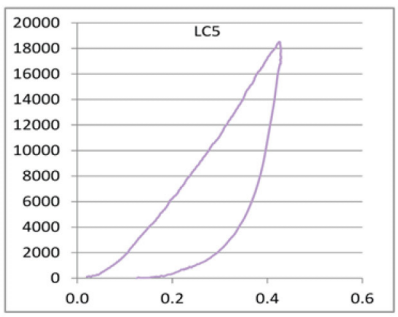
LC5
20000
18000
16000
14000
12000
10000
8000
6000
4000
2000
0
0.0
0.2
0.4
0.6

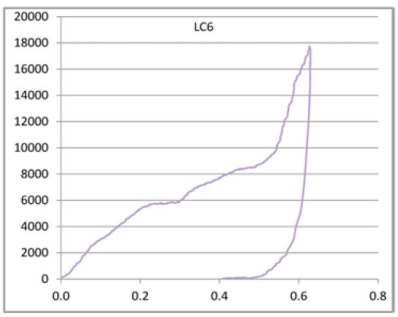
LC6
20000
18000
16000
14000
12000
10000
8000
6000
4000
2000
0
0.0
0.2
0.4
0.6
0.8

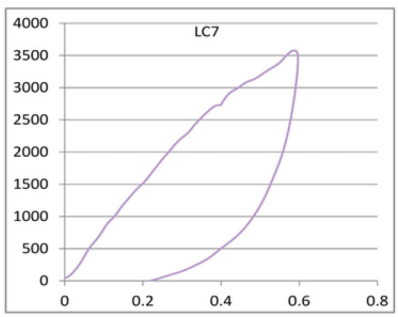
LC7
4000
3500
3000
2500
2000
1500
1000
500
0
0
0.2
0.4
0.6
0.8

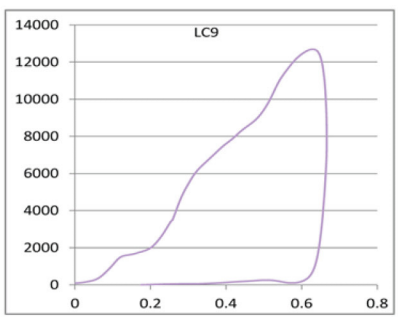
LC9
14000
12000
10000
8000
6000
4000
2000
0
0
0.2
0.4
0.6
0.8

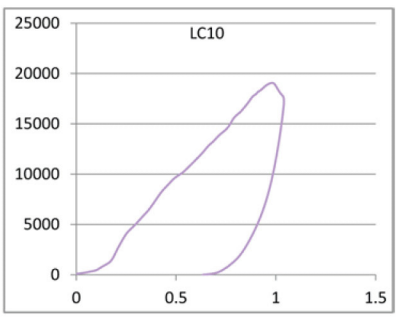
LC10
25000
20000
15000
10000
5000
0
0
0.5
1
1.5

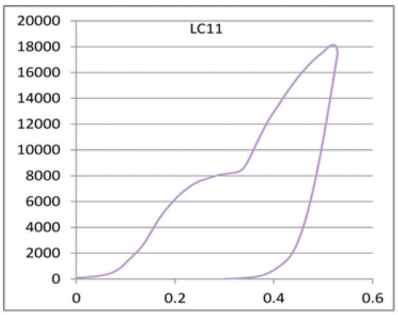
LC11
20000
18000
16000
14000
12000
10000
8000
6000
4000
2000
0
0
0.2
0.4
0.6

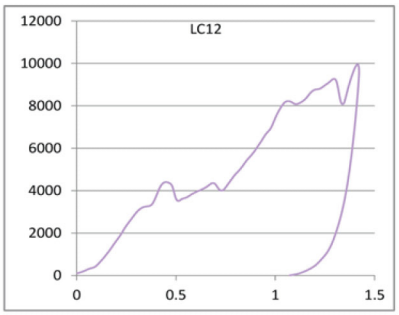
LC12
12000
10000
8000
6000
4000
2000
0
0
0.5
1
1.5

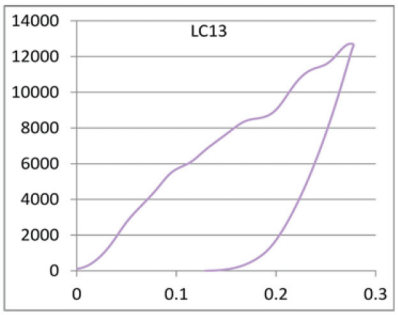
LC13
14000
12000
10000
8000
6000
4000
2000
0
0
0.1
0.2
0.3

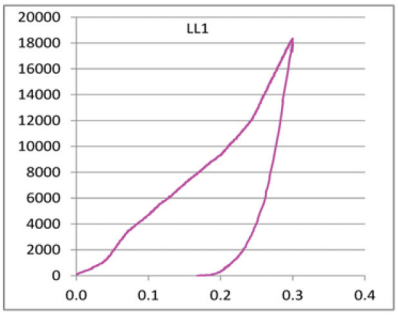
LL1
20000
18000
16000
14000
12000
10000
8000
6000
4000
2000
0
0.0
0.1
0.2
0.3
0.4

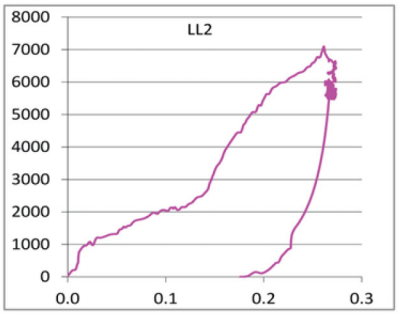
LL2
8000
7000
6000
5000
4000
3000
2000
1000
0
0.0
0.1
0.2
0.3

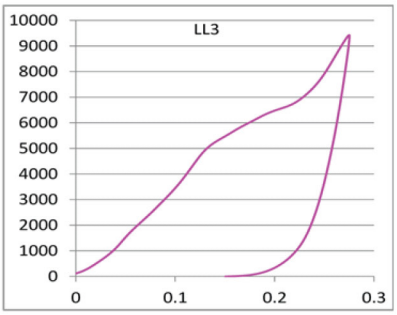
LL3
10000
9000
8000
7000
6000
5000
4000
3000
2000
1000
0
0
0.1
0.2
0.3

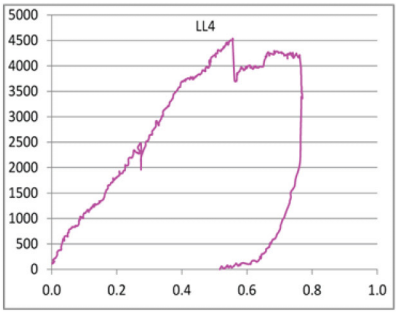
LL4
5000
4500
4000
3500
3000
2500
2000
1500
1000
500
0
0.0
0.2
0.4
0.6
0.8
1.0

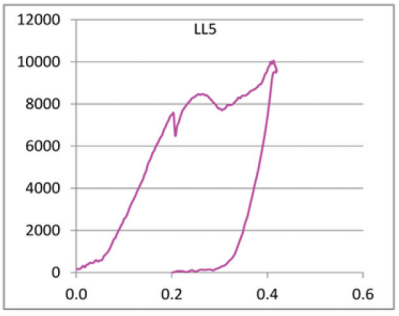
LL5
12000
10000
8000
6000
4000
2000
0
0.0
0.2
0.4
0.6

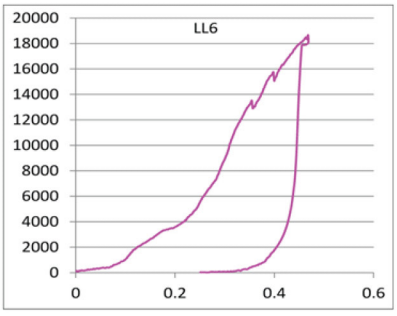
LL6
20000
18000
16000
14000
12000
10000
8000
6000
4000
2000
0
0
0.2
0.4
0.6

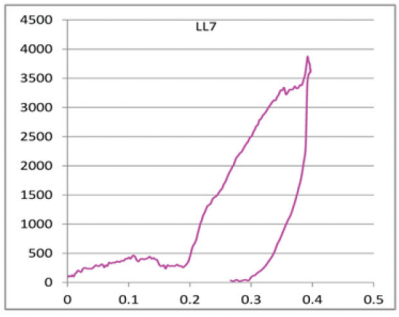
LL7
4500
4000
3500
3000
2500
2000
1500
1000
500
0
0
0.1
0.2
0.3
0.4
0.5

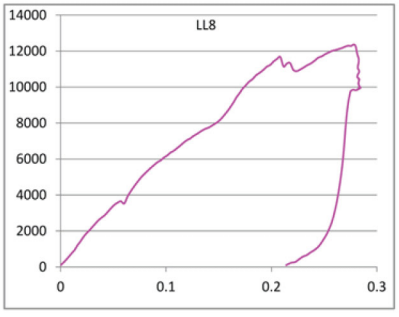
LL8
14000
12000
10000
8000
6000
4000
2000
0
0
0.1
0.2
0.3

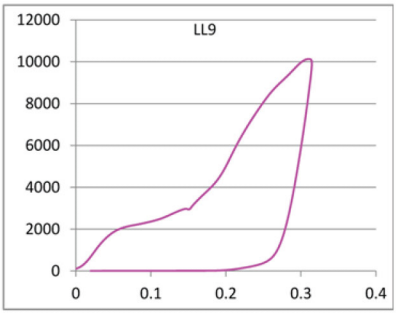
LL9
12000
10000
8000
6000
4000
2000
0
0
0.1
0.2
0.3
0.4

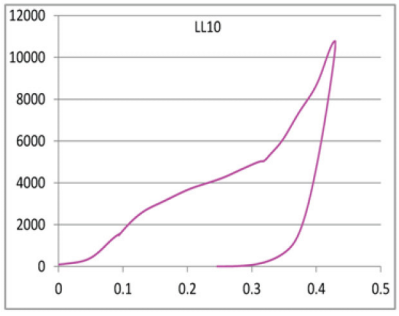
LL10
12000
10000
8000
6000
4000
2000
0
0
0.1
0.2
0.3
0.4
0.5

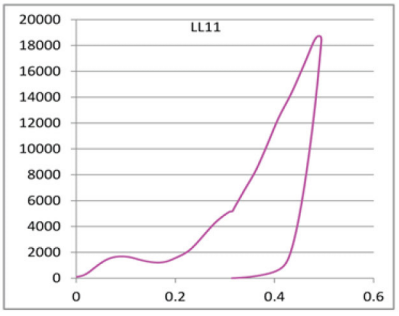
LL11
20000
18000
16000
14000
12000
10000
8000
6000
4000
2000
0
0
0.2
0.4
0.6

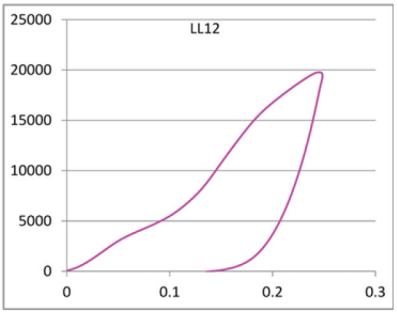
LL12
25000
20000
15000
10000
5000
0
0
0.1
0.2
0.3